Bioorganic & Medicinal Chemistry Letters 20 (2010) 157–160

Contents lists available at ScienceDirect

Bioorganic & Medicinal Chemistry Letters

journal homepage: www.elsevier.com/locate/bmcl

The discovery of tetrahydro-β-carbolines as inhibitors of the kinesin Eg5

Paul A. Barsanti *, Weibo Wang, Zhi-Jie Ni, David Duhl, Nathan Brammeier, Eric Martin, Dirksen Bussiere, Annette O. Walter

Global Discovery Chemistry/Oncology and Exploratory Chemistry, Novartis Institutes for Biomedical Research, 5400 Hollis Street, Emeryville, CA 94608, USA

ARTICLE INFO

Article history:
Received 15 September 2009
Revised 30 October 2009
Accepted 5 November 2009
Available online 12 November 2009

Keywords:
Eg5
KSP
Kinesin

ABSTRACT

A series of tetrahydro-β-carbolines were identified by HTS as inhibitors of the kinesin Eg5. Molecular modeling and medicinal chemistry techniques were employed to explore the SAR for this series with a focus of removing potential metabolic liabilities and improving cellular potency.

Eg5 is a member of the kinesin family of proteins, which hydrolyze ATP as they migrate along microtubules. Kinesins play pivotal roles in chromosome motility, spindle assembly/function, and in the transport of vesicles and organelles.[1] Eg5 (also known as Kinesin-5, BimC, KIF11, KSP) is essential in mitosis, and is expressed primarily in dividing cells. Inhibition of Eg5 blocks centrosome separation and thereby inhibits cell division. Current anti-mitotic drugs stop cell division through direct effects on microtubule stability. Eg5 inhibition, on the other hand, blocks mitosis by preventing spindle formation without directly affecting microtubule dynamics. Eg5 inhibitors are specific to dividing cells, and thus lack the neuronal toxicity of taxanes and vinca alkaloids.[2] Eg5 and its inhibitors have been the subject of several reviews.[3] We describe herein the discovery of potent tetrahydro-β-carboline inhibitors of Eg5 that were identified from optimization of high-throughput screening (HTS) hits.

Synthesis of the tetrahydro-β-carbolines began with Fisher Indole synthesis utilizing the bis-ethoxy acetal **1** which followed by phthalimide deprotection afforded the tryptamine derivatives (Scheme 1). Subjection of the tryptamines with aldehydes under standard Pictet–Spengler conditions afforded the corresponding tetrahydro-β-carbolines in good yields. Acylation followed by Boc-deprotection afforded the final compounds in excellent yields.[4]

Concurrent to our internal fast-follower[5] Eg5 program, we also ran an Eg5 HTS assay in order to pursue potentially more diverse chemotypes. Our primary Eg5 screening assay employed a standard ATPase assay.[6a] Our HTS efforts yielded several intriguing

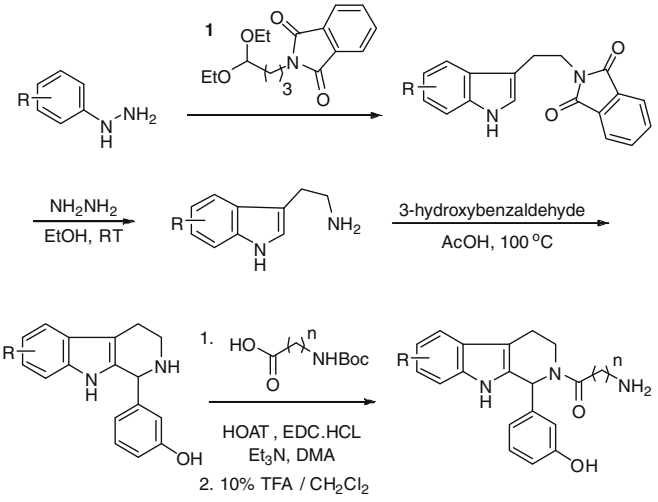

Scheme 1. Synthesis of *N*-acyl-tetrahydro-β-carbolines.

chemotypes, one of which was the tetrahydro-β-carboline (TH-β-carboline) **2**, which had an Eg5 IC_{50} of 2.5 μM (Fig. 1). Shortly thereafter, it was found that addition of a single methyl group in the aryl ring to give compound **3** led to a 10-fold increase in Eg5 binding affinity. In conjunction with our internal Eg5 co-crystallography efforts in our pyrimidinone series, we were successful in obtaining a co-crystal structure[7] of **3**, which induces a new pocket as it did for the pyrimidinone series[8] (Fig. 2a). This is consistent with all reported co-crystal structures in the PDB which show similar

* Corresponding author.
E-mail address: paul.barsanti@novartis.com (P.A. Barsanti).

0960-894X/$ - see front matter © 2009 Elsevier Ltd. All rights reserved.
doi:10.1016/j.bmcl.2009.11.012

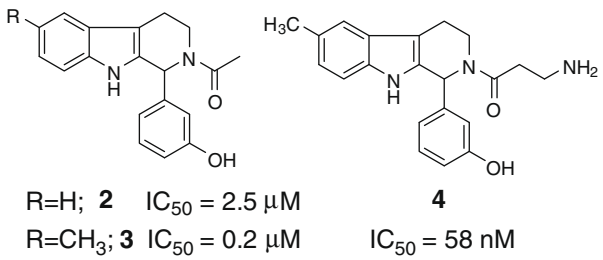

Figure 1. Lead series evolution.

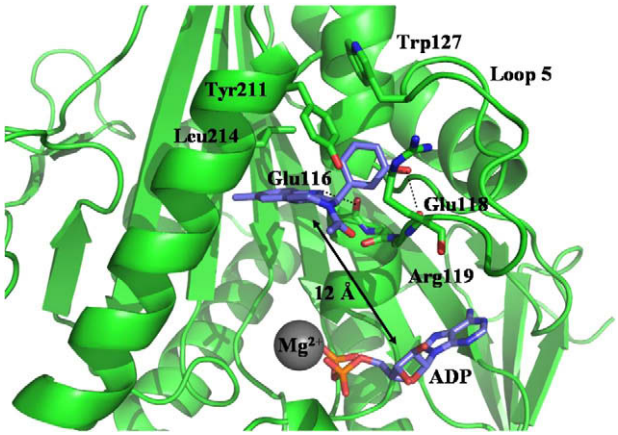

Figure 2a. Co-crystal structure of **3** bound to Eg5; Phenol of carboline displaces sidechain of Tyr211 to a new position. Loop 5 translocates approximately 10 A to form the top of the pocket.

structural movements in the protein upon binding compounds in the same allosteric site.[9]

There is a strong hydrogen bond between the phenolic –OH and the backbone carbonyl of Glu118, and worth about 10× in potency relative to –H or 100× relative to –Me. Additional possible hydrogen bonds from the carboline –NH and amide carbonyl have suboptimal geometries and are inconsistent from analog to analog, suggesting that most of the binding is hydrophobic (Fig. 2b).

Interestingly, although compound **3** was soaked into the crystal as the racemic mixture, it is the R enantiomer that the protein selects. Following modeling overlays with our potent in-house pyrimidinone series of Eg5 inhibitors, an amino functionality was introduced in an attempt to pick up additional hydrogen bonds to Glu215 or Tyr211, leading to the TH-β-carboline **4** whereby the acetyl moiety has been chain extended to terminate with a

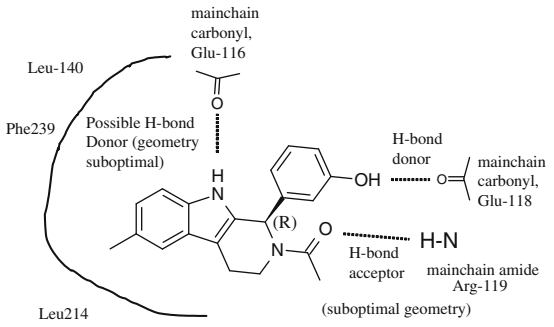

Figure 2b. Schematic depicting key interactions in co-crystal structure of **3** bound in an allosteric site of Eg5.

Table 1
SAR of the aryl ring for compounds **5–14**

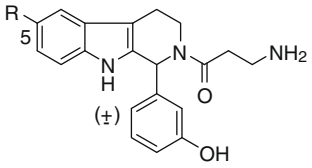

Compound[a]	R	Eg5 IC_{50} (μM)	Cell GI_{50} (μM)
5	H	0.63	n.d.
6	F	0.76	n.d.
7	Me	0.020	0.13
8	Et	0.011	0.10
9	^{i}Pr	>25	n.d.
10	Ph	1.7	n.d.
11	Cl	0.039	0.525
12	Br	0.027	0.496
13	OH	4.5	n.d.
14	CF_3O	0.2	>2

n.d., not determined.
[a] All compounds tested as racemic mixtures.

basic primary amine. Although these interactions were never confirmed by X-ray, this did lead to a substantial increase in binding affinity to Eg5.

The combination of ease of synthesis, rapid increase in potency and the ability to embark on a structure based drug design program encouraged us to explore the structure–activity relationship (SAR) of compounds in this series. It was apparent from early SAR that hydrophobic groups in the fifth position of the β-carboline nucleus were optimal and followed the trend of Et > Me ~ Br > Cl in binding affinity, however, the Cl and Br had poor cell activity (Table 1). In addition, di-substitution was not well tolerated by the active site.

With these data in hand, we turned our attention to the effect of the amine sidechain, the results of which are summarized in Table 2. In varying the length of the sidechain, we found that a two carbon tether is optimal in the acyclic series, consistent with modeling. In general, a 4–5-fold difference in potency was noted between the biochemical and cellular assays. Notably, compound **20** demonstrated similar potency in both biochemical and cell assays. Deletion of the amine as in compound **15** resulted in a greater than 10-fold loss in binding affinity. Replacement of the amide carbonyl to a sulfonamide linkage such as in compound **19** resulted in approximately a 10-fold loss in Eg5 binding affinity. The loss in potency observed in capping the basic amine such as in the sulfonamide **23** is consistent with the observations from modeling of the co-crystal structures in that the amine is involved in a key hydrogen bond.

In order to try to pick up further hydrophobic interactions, various alkyl substituents were introduced proximal to the amine. Interestingly, the enzyme distinguishes between the two different diastereoisomers **24** and **25**.

As part of the hit-to-lead process, we sought to identify any issues that might arise from the pharmacokinetic profile, especially since the series contained a phenol, a well known potential metabolic liability. Indeed, the rat PK of **4** confirmed our suspicions since it exhibited high clearance and no oral bioavailability (Table 3), whilst the direct phenyl analogue **26** had much improved PK properties.

To this end, we investigated phenol replacements (Table 4). Modeling suggested that cyclohexyl would be a suitable replacement, and indeed whilst better than most, it still exhibited a

Table 2
Sidechain SAR

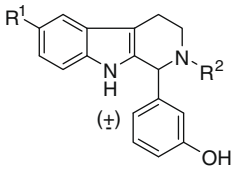

Compound[a]	R^1	R^2	Eg5 IC_{50} (μM)[b]	HCT-116 EC_{50} (μM)[b]
15	CH_3		0.46	1.4
16	CH_3	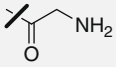	0.049	0.25
17	CH_3	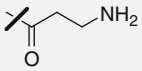	0.020	0.083
18	CH_3	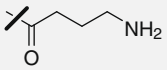	0.086	0.43
19	Cl	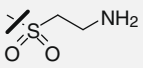	0.186	0.256[c]
20	CH_3	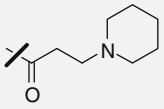	0.10	0.07
21	CH_3	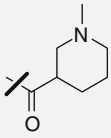	0.9	2.0[d]
22	Cl	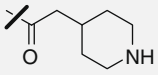	0.86	>2.0[d]
23	Cl	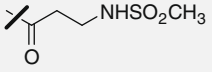	0.155	0.87[e]
24[f]	Cl	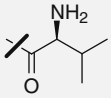	0.76	n.d
25[f]	Cl	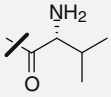	8.1	n.d

n.d., not determined.
[a] All compounds tested as racemic mixtures.
[b] See Refs. 6a,b for assay details.
[c] COLO-205 cell line.
[d] KB3.1 cell line.
[e] MDA-MB-435 cell line.
[f] Approximately 1:1 mixture of diastereoisomers.

Table 3
Rat PK

Compound	$T_{½}$ (h)	Cl (mL/min/kg)	Vd_{ss} (L/kg)	%F
4	10.7	171	94	1
26	9.5	26	18	32

10-fold loss in Eg5 binding affinity. The 3-fluorophenyl **33** turned out to be a reasonable replacement with only a modest decrease in binding affinity.

Table 4
Phenol replacements

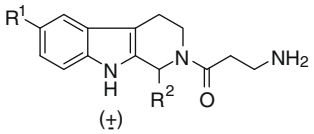

Compound[a]	R^1	R^2	Eg5 IC_{50} (μM)
26	CH_3		0.175
27	CH_3	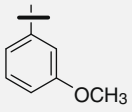	11.0
28	CH_3	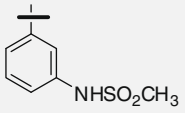	>25
29	CH_3	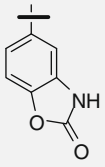	>25
30	Cl	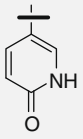	>25
31	Cl	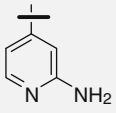	6.6
32	Cl	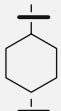	0.23
33	CH_3	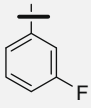	0.10

[a] All compounds tested as racemic mixtures.

In order to establish that the observed cellular activity was indeed through Eg5 inhibition, we initiated several mechanistic studies. U2OS cells were left untreated or treated with compound **3** at 1 μM for 8 h before being stained with DAPI (DNA) and an anti-β-tubulin antibody (β-tubulin).

Representative pictures of normal (bipolar spindle) and abnormal (mono-polar spindle) mitotic figures are shown (Fig. 3). Compound **3** has no effect on microtubules in the interphase, and demonstrates the mono-polar spindle formation in mitosis which is the phenotypic signature of Eg5 inhibition.

In summary, we have identified a novel class of small molecule Eg5 inhibitors. These inhibitors were potent in the biochemical assays, and demonstrated activity in cells consistent with the expected mechanism of action. The phenolic metabolic liability was replaced with a phenyl group which greatly improved the PK properties of the series. Further optimization of this series will be reported in due course.

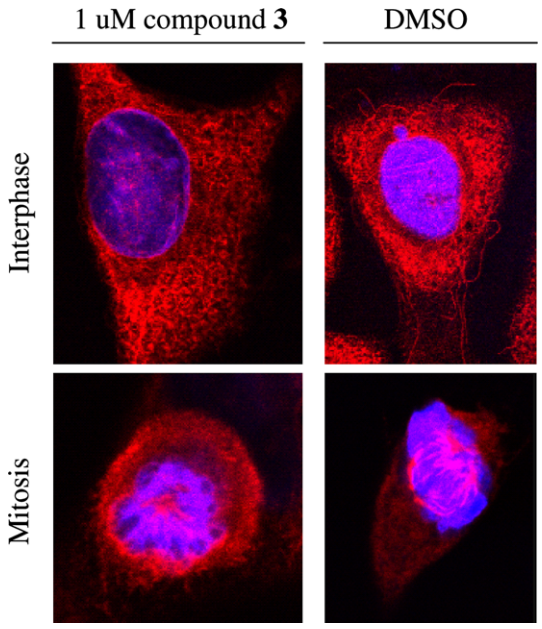

Figure 3. U2OS cells were treated with compound **3** at 1 μM for 8 h. Chromosomes are visualized using DAPI staining (blue) and microtubules are visualized using β-tubulin antibodies (red).

Acknowledgments

We thank Vincent Le and Cornelia Bellamacina for their help in collecting and interpreting the crystallographic data.

References and notes

1. Endow, S. A. *BioEssays* **2003**, *25*, 1212.
2. Chu, Q. S .; Holen, K. D.; Rowinsky, E. K.; Wilding, G.; Volkman, J. L.; Orr, J. B.; Williams, D. D.; Hodge, J. P.; Sabry, J. 40th ASCO Annual Meeting, New Orleans, LA, USA, 2004, 22(14S), Abs 2078.
3. (a) Zhang, Y.; Xu, W. *Anti-Cancer Agents Med. Chem.* **2008**, *8*, 698; (b) Jiang, C.; You, Q.; Li, Z.; Guo, Q. *Exp. Opin. Ther. Patents* **2006**, *16*, 1517.
4. For detailed experimental procedures see Wang, W.; Ni, Z.; Barsanti, P.; Pecchi, S.; Xia, Y.; Brammeier, N.; Treutle, M.; Jazan, E.; Wayman, K.; Dibble, D.; Cheng, J. WO05070930, 2005.
5. (a) Wang, W.; Lagniton, L. M.; Constantine, R. N.; Burger, M. T. WO04111058, 2004.; (b) Wang, W.; Constantine, R. N.; Lagniton, L. M.; Pecchi, S.; Burger, M. T.; Desai, M. C. WO04113335, 2004.
6. (a) Purified Eg5 enzyme is put into solution at 3 nM along with 50 μg/ml purified bovine brain tubulin, 250 μM ATP, and inhibitors of Eg5 in a final concentration of 2.5% DMSO. The assay is incubated for 2 h.; (b) The compounds anti-proliferative activity on cells was assessed by determining the concentration of inhibitor that results in 50% growth inhibition (GI_{50}, using CellTiter-Glo® to measure ATP) after 72 h incubation.
7. The coordinates have been deposited with RCSB Protein Data Bank under accession code 3K3B.
8. Wang, W.; Constantine, R.; Lagniton, L. US05228002, 2005.
9. (a) Yan, Y.; Sardana, V.; Xu, B.; Homnick, C.; Halczenko, W.; Buser, C. A.; Schaber, M.; Hartman, G. D.; Huber, H. E.; Kuo, L. C. *J. Mol. Biol.* **2004**, *335*, 547; (b) Cox, C. D.; Breslin, M. J.; Mariano, B. J.; Coleman, P. J.; Buser, C. A.; Walsh, E. S.; Hamilton, K.; Huber, H. E.; Kohl, N. E.; Torrent, M.; Yan, Y.; Kuo, L. C.; Hartman, G. D. *Bioorg. Med. Chem. Lett.* **2005**, *15*, 2041; (c) Cox, C. D.; Torrent, M.; Breslin, M. J.; Mariano, B. J.; Whitman, D. B.; Coleman, P. J.; Buser, C. A.; Walsh, E. S.; Hamilton, K.; Schaber, M. D.; Lobell, R. B.; Tao, W.; South, V. J.; Kohl, N. E.; Yan, Y.; Kuo, L. C.; Prueksaritanont, T.; Slaughter, D. E.; Li, C.; Mahan, E.; Lu, B.; Hartman, G. D. *Bioorg. Med. Chem. Lett.* **2006**, *16*, 3175; (d) Tarby, C. M.; Kaltenbach, R. F.; Huynh, T.; Pudzianowski, A.; Shen, H.; Ortega-Nanos, M.; Sheriff, S.; Newitt, J. A.; McDonnell, P. A.; Burford, N.; Fairchild, C. R.; Vaccaro, W.; Chen, Z.; Borzilleri, R. M.; Naglich, J.; Lombardo, L. J.; Gottardis, M.; Trainor, G. L.; Roussell, D. L. *Bioorg. Med. Chem. Lett.* **2006**, *16*, 2095.